Journal of Colloid and Interface Science 364 (2011) 112–117

Contents lists available at SciVerse ScienceDirect

Journal of Colloid and Interface Science

www.elsevier.com/locate/jcis

Hollow capsules prepared from all block copolymer micelle multilayers

Jinkee Hong [a,1], Jinhan Cho [b,*], Kookheon Char [a,*]

[a] Intelligent Hybrids Research Center, School of Chemical and Biological Engineering, The WCU Program of Chemical Convergence for Energy & Environment, Seoul National University, Seoul 151-744, Republic of Korea
[b] Department of Chemical and Biological Engineering, Korea University, Anam-dong, Seongbuk-gu, Seoul 136-713, Republic of Korea

ARTICLE INFO

Article history:
Received 15 June 2011
Accepted 3 August 2011
Available online 22 August 2011

Keywords:
Hollow capsule
Micelle
Block copolymer
Layer-by-layer
Multilayer

ABSTRACT

We introduce a novel and versatile approach for preparing hollow multilayer capsules containing functional hydrophobic components. Protonated polystyrene-*block*-poly(4-vinylpyridine) (PS-*b*-P4VP) and anionic polystyrene-*block*-poly(acrylic acid) (PS-*b*-PAA) block copolymer micelles (BCM) were used as building blocks for the layer-by-layer assembly of BCM multilayer films onto polystyrene (PS) colloids. After removing the PS colloids, the stabilities of the formed BCM hollow capsules were found to be strongly dependent on the charge density of the hydrophilic corona segments (i.e., P4VP and PAA block segments) as well as the relative molecular weight ratio of hydrophobic core (i.e., PS segments) blocks and hydrophilic corona shells. Furthermore, in the case of incorporating hydrophobic fluorescent dyes into the PS core blocks of micelles, the hairy/hairy BCM multilayers showed well-defined fluorescent images after colloidal template removal process. These phenomena are mainly caused by the relatively high degree of electrostatic interdigitation between the protonated and anionic corona block shells.

1. Introduction

Hollow capsules consisting of organic [1,2], inorganic [3], or organic–inorganic composites [4] have attracted considerable attention over the past few years due to their potential applications in drug delivery, artificial cells, catalysis, and optical sensing. Efforts to prepare hollow capsules have mainly focused on polymerization, oxidation-etching methods, hydrothermal-calcination treatment, and interface assembly on sacrificial substrates, liquid droplets or microemulsion droplets [5–11]. Although these approaches can provide simple and facile routes for preparing hollow capsules, they are typically driven by their ability to process selective organic or inorganic components coupled with their high affinity to sacrificial substrates. Consequently, it is difficult to prepare hollow films with a well-defined but varied thickness and integrated chemical composition with nanometer precision using these methods. Furthermore, it is not possible to easily incorporate hydrophobic functional components into the aqueous solution based processes.

The layer-by-layer (LbL) assembly method offers a variety of opportunities to fabricate thin films with desired functional properties. An important advantage of this method lies in the fact that it enables the preparation of films with tailored film thickness, composition, functionality on sacrificial substrates of different size and shape [4,12–16]. In addition, various hydrophilic materials, ranging from conventional polyelectrolytes to biomaterials or inorganic nanoparticles, can be incorporated within the LbL films through complementary interactions (i.e., electrostatic [12,13,17,18], hydrogen-bonding [19–23] or covalent interactions [24,25]). Recently, it has been reported that block copolymer micelles (BCMs) consisting of hydrophilic and hydrophobic block segments, such as polystyrene-*b*-poly(acrylic acid) (PS-*b*-PAA), can be used to encapsulate hydrophobic materials (e.g., gold [26,27], magnetic nanoparticles [28] or fluorescent dyes [29,30]) into the hydrophobic core of micelles followed by the chemical crosslinking of the corona shells. More recently, we have demonstrated that LbL-assembled BCM/polyelectrolyte [29,31] or BCM/BCM multilayers containing hydrophobic segments could be successfully prepared in aqueous solution onto both flat [32,33] and colloidal substrates [34,35] based on the electrostatic and/or hydrogen bonding interactions. These findings prompt intriguing new possibilities for functional hollow capsules to allow the incorporation of both hydrophilic and hydrophobic components into a multilayered film.

This paper reports the preparation of hollow BCM capsules, which were assembled utilizing the electrostatic and hydrogen-bonding interactions between different BCMs (cationic polystyrene-*block*-poly(4-vinylpyrine) (PS-*b*-P4VP) and anionic polystyrene-*block*-poly(acrylic acid) (PS-*b*-PAA)). These BCMs were

* Corresponding authors.
E-mail addresses: jinhan71@korea.ac.kr (J. Cho), khchar@plaza.snu.ac.kr (K. Char).
[1] Present address: Department of Chemical Engineering, Massachusetts Institute of Technology, Cambridge, MA 02139, USA.

0021-9797/$ - see front matter © 2011 Elsevier Inc. All rights reserved.
doi:10.1016/j.jcis.2011.08.012

also used to incorporate hydrophobic fluorescent dyes (e.g., water-insoluble fluorescent nile-red and coumarin 30 dyes) into the individual PS micellar cores, allowing the control of optical properties of the films. The stability of hollow capsule prepared by PS-*b*-P4VP/PS-*b*-PAA multilayers was adjusted by varying the molecular weights (M_W) of the hydrophobic core (PS). For this study, LbL multilayers prepared with (*hairy BCM* with relatively long hydrophilic chains/hairy BCM)$_{n\ (n=\text{number of bilayer})}$, (*crew-cut BCM* with relatively short hydrophilic chains/crew-cut BCM)$_n$, and (crew-cut BCM/hairy BCM)$_n$ pairs were prepared. Using the three different types of BCM pairs for the multilayer deposition, we demonstrate that the relative ratio of M_W between the hydrophobic core and hydrophilic corona as well as the degree of interdigitation or entanglements between the P4VP and PAA corona chains of BCMs (e.g., hairy/hairy BCM, crew-cut/hairy BCM and crew-cut/crew-cut BCM multilayers) has a significant effect on the physical and chemical stability of hollow capsules containing hydrophobic dyes. Consequently, the significance of this study lies in the fact that the BCM multilayer capsules obtained in this study based on the electrostatic interactions can easily control their stability after PS colloidal substrate removal through physical variables (i.e., the molecular weight (M_W) of BCM blocks and degree of interdigitation or entanglement between two different corona chains) without additional chemical crosslinking. This approach could also provide a basis for constructing hollow capsules requiring the insertion of a range of functional components.

2. Experimental

2.1. Materials

$PS_{(Mw=10.6K)}$-*b*-$P4VP_{(Mw=42.4K)}$ ($PS_{10.6K}$-*b*-$P4VP_{42.4K}$) block copolymers was synthesized using anionic polymerization, as previously reported [57]. Other block copolymers (e.g., $PS_{4.3K}$-*b*-$PAA_{19.5K}$, PS_{2K}-*b*-PAA_{8K}, PS_{1K}-*b*-$PAA_{40.2K}$, PS_{16K}-*b*-PAA_{4K}, $PS_{18.6K}$-*b*-$P4VP_{55.8K}$, PS_{124K}-*b*-$P4VP_{42K}$, PS_{480K}-*b*-$P4VP_{145K}$ and $PS_{49.5K}$-*b*-$P4VP_{16.5K}$), water-insoluble fluorescent dyes (e.g., nile red and coumarin 30) and sulfate-stabilized PS colloids (600 nm and 2 μm) were purchased from Polymer Source, Sigma Aldrich and Microparticles GmbH, respectively.

2.2. Preparation of block copolymer micelles

For the preparation of protonated PS-*b*-P4VP micelles in water, 50 mg of PS-*b*-P4VP block copolymer was first dissolved in 2 mL of mixed organic solvents (N,N-dimethylformamide (DMF) and tetrahydrofuran (THF) by volume ratio). Subsequently, 48 mL of water (pH 2.0) was added dropwise to produce spherical micelles composed of a hydrophobic PS core and a protonated P4VP corona shell. As water was further added, the solution gradually turned into a light milky suspension, indicating the formation of micelle suspension. After stirring for 3 h, the resulting suspension was subjected to the dialysis against Millipore water for over 24 h (Spectra/Por® 4 Regenerated Cellulose Membrane, MWCO = 12–14 K) to remove any residual organic solvent. After forming PS-*b*-P4VP micelles at pH 2, the pH of the PS-*b*-P4VP micelle solutions was adjusted to the desired solution pH using 0.1 M NaOH. In contrast, PS-*b*-PAA (50 mg) in 2 mL DMF/THF was dissolved in 48 mL of water at pH 10 to prepare the anionic PS-*b*-PAA BCMs. The pH of the PS-*b*-PAA micelle solution was then controlled using 0.1 M HCl. The silicon wafers, quartz glass, and glass substrates were cleaned initially with a Piranha solution (sulfuric acid/hydrogen peroxide = 70/30 v/v%), and then charged negatively by heating at 70 °C for 20 min in a 5:1:1 vol% mixture of water, hydrogen peroxide and a 29% ammonia solution (RCA solution).

2.3. Preparation of BCM multilayers on colloids

The concentration of BCM solutions used in all the deposition experiments was fixed at 1 mg mL^{-1} without ionic salt. The PS-*b*-P4VP/PS-*b*-PAA multilayer-coated polystyrene colloids were prepared as follows: 100 μL of a concentrated dispersion (6.4 wt%) of negatively charged polystryene colloids was diluted to 0.5 mL with deionized water. Subsequently, 0.5 mL of PS-*b*-P4VP (1 mg mL^{-1} at pH 4) was added. After deposition for 10 min, the excess PS-*b*-P4VP BCMs were removed by three centrifugation (8000 rpm at 4 °C for 5 min)/wash cycles. PS-*b*-PAA (1 mg mL^{-1} at pH 4) BCMs was then allowed to deposit on the PS-*b*-P4VP-coated PS colloids under the same conditions. The above process was repeated until three bilayers of PS-*b*-P4VP/PS-*b*-PAA have been deposited onto polystyrene colloids. In order to incorporate water-insoluble fluorescent dyes into the BCMs, 0.08 mg of coumarin 30 and 0.06 mg of nile red were mixed in $PS_{4.3K}$-*b*-$PAA_{19.5K}$ (1 mg mL^{-1} in 2 mL DMF/THF) and $PS_{18.6K}$-*b*-$P4VP_{55.8K}$ (1 mg mL^{-1} in 2 mL DMF/THF) solutions, respectively. Subsequently, 48 mL of deionized water was added slowly with vigorous stirring. The fluorescence dye-incorporated micelle solutions were subject to dialysis against Millipore water for over 24 h (Spectra/Por® 4 Regenerated Cellulose Membrane, MWCO = 12–14 K) to remove any excess dyes and residual organic solvent.

2.4. UV–Vis spectroscopy

The UV–Vis spectra were obtained using a Perkin Elmer Lambda 35-UV–Vis spectrometer. The pyridine groups in the PS-*b*-P4VP showed the absorbance peak centered at 254 nm.

2.5. ζ-Potential measurements

The ζ-potentials of PS-*b*-P4VP and PS-*b*-PAA micelles were measured using an electrophoretic light scattering spectrophotometer (ELS-8000). The periodic changes in the ζ-potentials were confirmed during the alternate deposition of cationic PS-*b*-P4VP and anionic PS-*b*-PAA micelles onto colloidal polystyrene particles.

2.6. Scanning electron microscopy (SEM)

The surface morphology of the BCM multilayer-coated PS colloids was examined by Field-Emission SEM (JEOL JSM-7401F).

2.7. Transmission electron microscope (TEM)

Energy-filtered TEM (LIBRA 120, Carl Zeiss) was used to examine the structure of hollow capsules composed of PS-*b*-P4VP/PS-*b*-PAA BCM multilayers.

2.8. Confocal laser scanning microscopy (CLSM)

The CLSM images of the fluorescent dye-incorporated hollow capsules were taken using a Carl Zeiss-LSM510.

3. Results and discussion

PS-*b*-P4VP block copolymer forms positively charged micelles consisting of hydrophobic PS cores and protonated P4VP corona shells in solutions at pH < 5, even though they are water-insoluble due to the deprotonation of the P4VP block segments at pH > 5. On the other hand, PS-*b*-PAA forms anionic micelles because the carboxylic acid groups (e.g., COOH) in the PAA corona shells become charged (e.g., COO^-) with increasing solution pH (pK_a of PAA ~ 4.5). These phenomena indicate that PS-*b*-P4VP and PS-*b*-PAA BCMs

have the pH-dependent charge density as the typical characteristic of weak polyelectrolytes and their charge densities can be easily adjusted by the solution pH. According to the previous results, the pH 4/4 deposition condition for PS-*b*-P4VP/PS-*b*-PAA multilayer assembly has yielded more densely packed films compared with other pH deposition conditions enhancing the charge density of PS-*b*-PAA (pH > 4) and/or PS-*b*-P4VP (pH < 4). It should be noted that the BCM multilayers assembled at pH 4/6 combination have yielded highly nanoporous structure due to the electrostatic repulsion originating from the increased charge density of the PAA corona (i.e., degree of ionization of about 90% at pH 6). However, at pH 4/4, the degree of PS-*b*-PAA ionization was measured to be approximately 18%, while the pyridine groups in PS-*b*-P4VP had a charge density of approximately 42% (see Supporting information, Fig. S1) Considering that hollow capsules are the free-standing multilayers obtained after removing the colloidal templates, the solution pH affecting the charge densities of corona blocks and the resultant multilayer assembly (e.g., multilayer structure and the adsorbed amount of components) of BCMs could also be quite important in determining the stability of hollow capsules.

Table 1
Block molecular weights (M_W) of the block copolymer micelles used in present study.

Molecular characteristics of block copolymers	
Polysterene-*block*-poly(4-vinylpyridine) $PS_{(Mw)}$-*b*-$P4VP_{(Mw)}$	(18.6k)-*b*-(55.8)
	(124k)-*b*-(42k)
	(1k)-*b*-(40.2k)
Polysterene-*block*-poly(acrylic acid) $PS_{(Mw)}$-*b*-$PAA_{(Mw)}$	(2k)-*b*-(8k)
	(4.3k)-*b*-(19.5k)
	(16k)-*b*-(4k)

Based on the pH-dependent charge densities of BCMs, the effects of relative molecular weight ratio between hydrophobic core and hydrophilic corona blocks on the formation of multilayers placed on PS colloids and the resulting hollow capsules after removing the colloidal substrates were first examined. For this study, three different types of hairy (i.e., $PS_{18.6K}$-*b*-$P4VP_{55.8K}$, PS_{1K}-*b*-$PAA_{40.2K}$ and $PS_{4.3K}$-*b*-$PAA_{19.5K}$) and two different crew-cut BCMs (i.e., PS_{124K}-*b*-$P4VP_{42K}$ and PS_{16K}-*b*-PAA_{4K}) were employed for the LbL assembly (Table 1).

In the case of $PS_{18.6K}$-*b*-$P4VP_{55.8K}$/$PS_{4.3K}$-*b*-$PAA_{19.5K}$ multilayers with a hairy micelle pair prepared in the pH 4/4 deposition

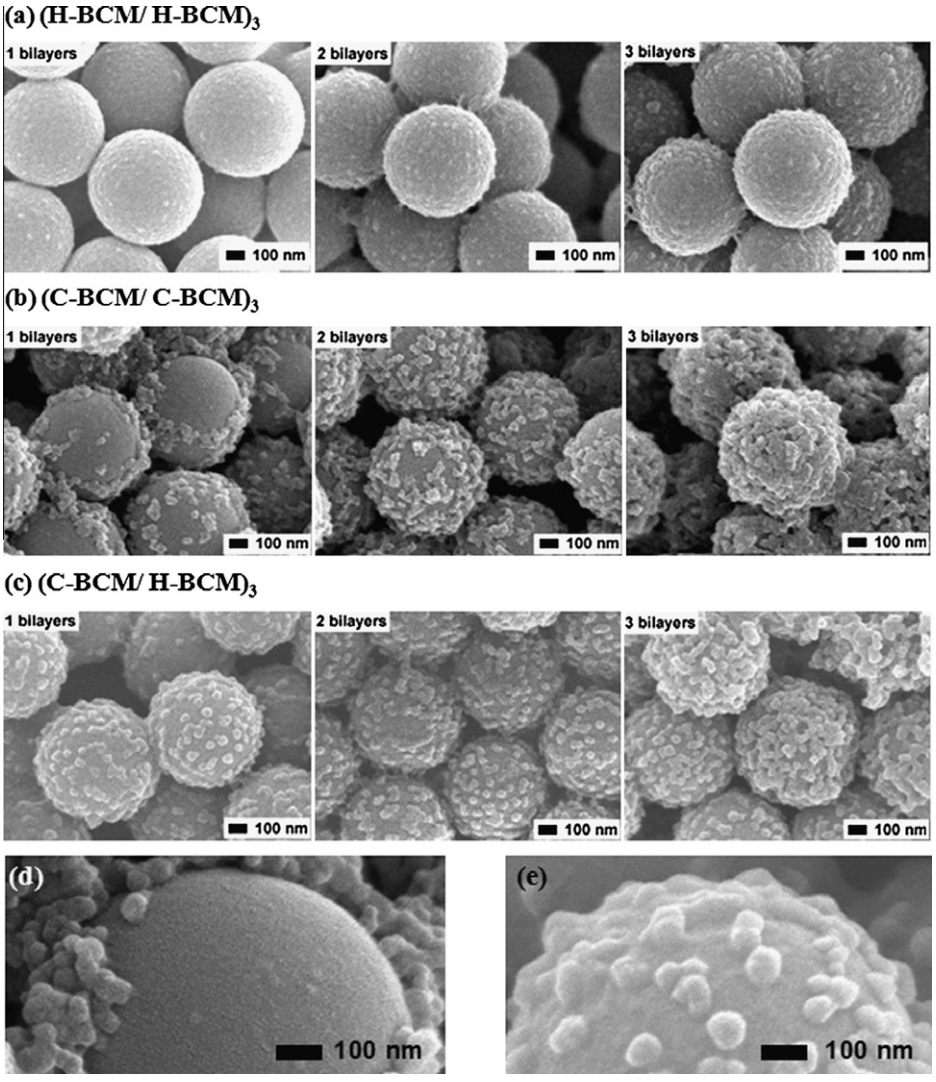

Fig. 1. SEM images of the surface morphologies of: (a) ($PS_{18.6K}$-b-$P4VP_{55.8K}$/$PS_{4.3K}$-b-$PAA_{19.5K}$)$_3$, (b) (PS_{124K}-b-$P4VP_{42K}$/PS_{16K}-b-PAA_{4K})$_3$ and (c) (PS_{124K}-b-$P4VP_{42K}$/$PS_{1.4K}$-b-$PAA_{40.2K}$)$_3$. All the BCM multilayers deposited onto PS colloids were prepared in the pH 4/4 deposition condition. (d) and (e) show the magnified images of the dashed regions in (b) and (c), respectively. In the figure, hairy and crew-cut BCMs were denoted as H-BCM and C-BCM, respectively.

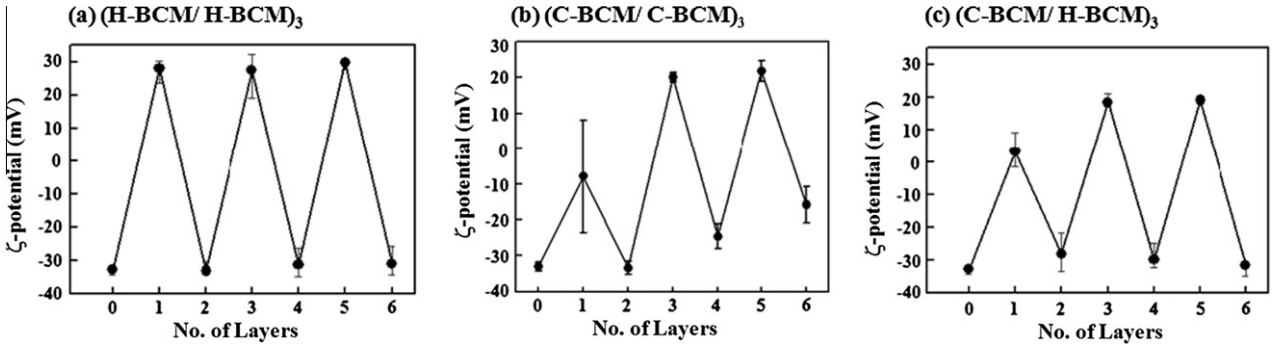

Fig. 2. Measured zeta-potentials of PS colloids alternatively coated with: (a) $PS_{18.6K}$-*b*-$P4VP_{55.8K}$ micelles (odd)/$PS_{4.3K}$-*b*-$PAA_{19.5K}$ micelles (even), (b) PS_{124K}-*b*-$P4VP_{42K}$ micelles (odd)/PS_{16K}-*b*-PAA_{4K} micelles (even), and (c) PS_{124K}-*b*-$P4VP_{42K}$ micelles (odd)/$PS_{1.4K}$-*b*-$PAA_{40.2K}$ micelles (even) in the pH 4/4 deposition condition as a function of layer number (hairy and crew-cut BCMs were denoted as H-BCM and C-BCM in the figure, respectively).

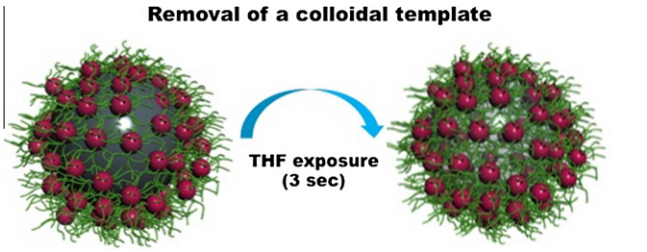

Fig. 3. A schematic showing of the preparation of BCM multilayered hollow capsules.

condition, the amount of hairy micelles adsorbed onto the PS colloids increases uniformly with increasing the bilayer number (Fig. 1a). The uniform adsorption of hairy micelles on the PS colloids from the first bilayer was also inferred from the measurements of zeta-potential periodically oscillating from +28 ± 2 mV (for $PS_{18.6K}$-*b*-$P4VP_{55.8K}$) to −33 ± 8 mV (for $PS_{4.3K}$-*b*-$PAA_{19.5K}$) (Fig. 2a). These results imply that a smooth and densely packed surface morphology shown in the hairy BCM multilayer-coated colloids, even in the first bilayer, can be obtained by the high degree of interdigitation or entanglement between relatively thick corona shells of $PS_{18.6K}$-*b*-$P4VP_{55.8K}$ and $PS_{4.3K}$-*b*-$PAA_{19.5K}$. On the other hand, the BCM multilayers consisting of oppositely charged crew-cut micelles (i.e., PS_{124K}-*b*-$P4VP_{42K}$ and PS_{16K}-*b*-PAA_{4K}) generate large vacancies on the colloidal surface despite the increase in the bilayer up to 2 (Fig. 1b). This SEM observation is also confirmed by the zeta-potential measurements showing a small amplitude oscillation from −8 ± 3 mV (for PS_{120K}-*b*-$P4VP_{42K}$) to −32 ± 8 mV (for PS_{16K}-*b*-PAA_{4K}) for the first bilayer adsorption before a rather irregular oscillations in zeta-potential as the bilayer number is increased (Fig. 2b). These results are believed to originate from the insufficient charge compensation with positively charged crew-cut micelles on negatively charged bare PS colloid templates as well as the low degree of electrostatic interdigitation or entanglement between P4VP and PAA corona chains with relatively low M_W compared to those of hydrophobic PS core blocks. As a result, it is quite likely that even three bilayered crew-cut/crew-cut micelle multilayers with seemingly sufficient surface coverage will also be vulnerable to external stimuli such as the removal of colloidal substrates and the swelling of hydrophobic PS blocks by organic solvent exposure. This is to say that the low degree of electrostatic interdigitation or entanglement between the micelle pairs can make it considerably difficult to generate stable free-standing forms, such as hollow capsules after removing the colloidal substrates (a detailed explanation will be given in the latter part). The surface morphology is also shown for the crew-cut/hairy micelle (i.e., PS_{124K}-*b*-$P4VP_{42K}$/$PS_{1.4K}$-*b*-$PAA_{40.2K}$) paired multilayers

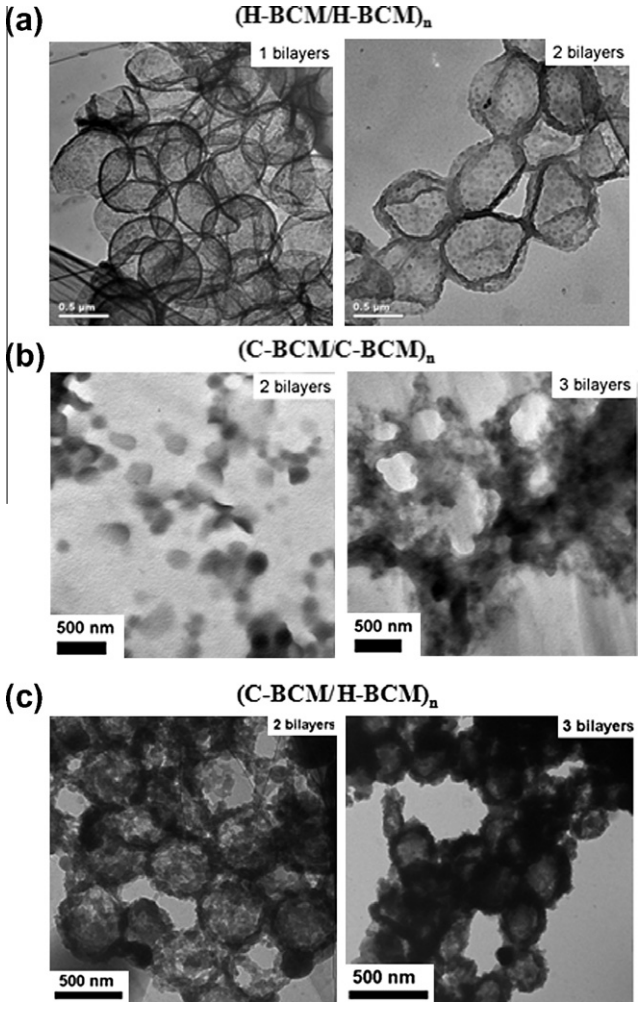

Fig. 4. TEM images of hollow capsules prepared from: (a) (pH 4 $PS_{18.6K}$-*b*-$P4VP_{55.8K}$/pH 4 $PS_{4.3K}$-*b*-$PAA_{19.5K}$)$_{n=1\text{ and }2}$, (b) (pH 4 PS_{124K}-*b*-$P4VP_{42K}$/pH 4 PS_{16K}-*b*-PAA_{4K})$_{n=2\text{ and }3}$, and (c) (pH 4 PS_{124K}-*b*-$P4VP_{42K}$/pH 4 $PS_{1.4K}$-*b*-$PAA_{40.2K}$)$_{n=2\text{ and }3}$. In the figure, hairy and crew-cut BCMs were denoted as H-BCM and C-BCM, respectively.

(Fig. 1c). Considering the fact that the hairy micelles with relatively small hydrophobic PS cores can be uniformly deposited on a substrate, it is quite plausible that the crew-cut/hairy micelle pair could increase its surface coverage. on the colloidal substrates even with less dense bumpy surface textures. In this case, even a single bilayer with a crew-cut/hairy micelle pair represents the full coverage on the PS colloids compared with the crew-cut/

crew-cut micelle multilayer (Fig. 1d and e). The zeta-potential profile of the crew-cut/hairy micelle pair also shows the almost complete charge conversion behavior for each BCM deposition from the first bilayer due to the sufficient surface coverage on colloidal particles (Fig. 2c).

In order to test our hypothesis, hollow capsules containing hairy/hairy, crew-cut/crew-cut, and crew-cut/hairy micelle paired multilayers were prepared after removing the sacrificial PS colloidal substrates by exposure to tetrahydrofuran (THF), as schematically shown in Fig. 3.

In this case, the hairy/hairy micelle multilayers prepared in the pH 4/4 deposition condition yielded hollow capsules with small dimples on the surface and the well-sealed capsule structure after removing the PS colloidal templates is quite similar to the structure prepared with conventional polyelectrolytes (Fig. 4a). In particular, the formation of a hairy/hairy micelle paired capsule with a single bilayer suggests that a high degree of electrostatic interdigitation between oppositely charged hairy micelles generates densely packed multilayers, keeping the hollow shell structure physically stable against external stimuli (e.g., the removal of PS colloidal substrates and the swelling of hydrophobic PS core blocks by THF treatment). It is also important to note that when the same hairy micelle paired multilayers were deposited on the PS colloids at pH 4/6 deposition condition (in this case, the charge density of PAA corona chains increases from 18% at pH 4 to 90% at pH 6), the degree of intermicellar entanglements is relatively low, when compared with the case of pH 4/4 deposition, yielding less stable hollow capsules due to the long-range electrostatic repulsion between fully charged PAA corona chains even when the bilayer number is increased up to 3 (see Supporting information, Fig. S2). In contrast, the (crew-cut/crew-cut micelle)$_{n=1,\ 2\ \text{and}\ 3}$ multilayered films did not yield the well-defined hollow shells showing the physical disruption of micellar multilayers due to insufficient micellar entanglements between $P4VP_{42K}$ and PAA_{4K} corona chains during the removal of sacrificial PS colloids (Fig. 4b). In particular, although $PS_{49.5k}$-*b*-$P4VP_{16.5K}$/PS_{16K}-*b*-PAA_{4K} multilayers consisting of crew-cut/crew-cut micelles deposited on colloidal substrates seemingly yielded a densely packed structure after three bilayer deposition, the removal of colloidal substrates by THF treatment caused the disruption of micellar hollow capsules. In the case of combining hairy micelles (i.e., $PS_{1.4K}$-*b*-$PAA_{40.2K}$) with crew-cut micelles (i.e., PS_{124K}-*b*-$P4VP_{42K}$), we found that stable hollow capsules could be obtained after the 2 bilayer deposition (Fig. 4c). These results suggest that the high degree of intermicellar entanglements between hydrophilic corona block chains has a significant effect on the formation of stable hollow capsules. In addition, the phenomena described in the present study are consistent with those shown in other BCM multilayers (i.e., hairy/hairy, crew-cut/crew-cut and crew-cut/hairy micelle multilayers) with different molecular weights and compositions (see Supporting information, Figs. S3 and S4). Consequently, the degree of intermicellar entanglements between hydrophilic corona block chains highlights the physical stability of hollow capsules upon removal of colloidal templates by THF treatment.

Based on highly stable hollow shells prepared from the hairy/hairy micelle pairs, the stability of the BCM multilayers containing hydrophobic fluorescence dyes in their individual PS block cores was further investigated by optical microscopy. For this investigation, two different fluorescence dyes (nile-red with red emission and coumarin 30 with green emission) with negligible Föster energy transfer between the dyes incorporated into the PS core blocks of $PS_{18.6K}$-*b*-$P4VP_{55.8K}$ and $PS_{4.3K}$-*b*-$PAA_{19.5K}$, respectively (see Supporting information, Fig. S5). After dye incorporation into the BCM cores, BCM micelles containing two different fluorescence dyes in two different PS cores were deposited on the PS colloids in the pH 4/4 deposition condition. In this case, the resulting ($PS_{18.6K}$-*b*-$P4VP_{55.8K}$ with nile-red/$PS_{4.3K}$-*b*-$PAA_{19.5K}$ containing coumarin 30)$_3$ multilayers deposited on the PS colloids display both red and green fluorescent emissions depending on the excitation wavelength chosen (i.e., 547 nm for nile red and 400 nm for coumarin 30) (Fig. 5a and c). Moreover, the fluorescent images of hollow capsules obtained after the removal of PS colloids by THF treatment strongly support the hypothesis that the hairy/hairy BCM multilayers with a high degree of intermicellar entanglements between oppositely charged corona block chains can increase the physical stability of hollow capsules upon THF treatment (Fig. 5d and f). Furthermore, considering the fact that both nile-red and coumarin 30 dyes are

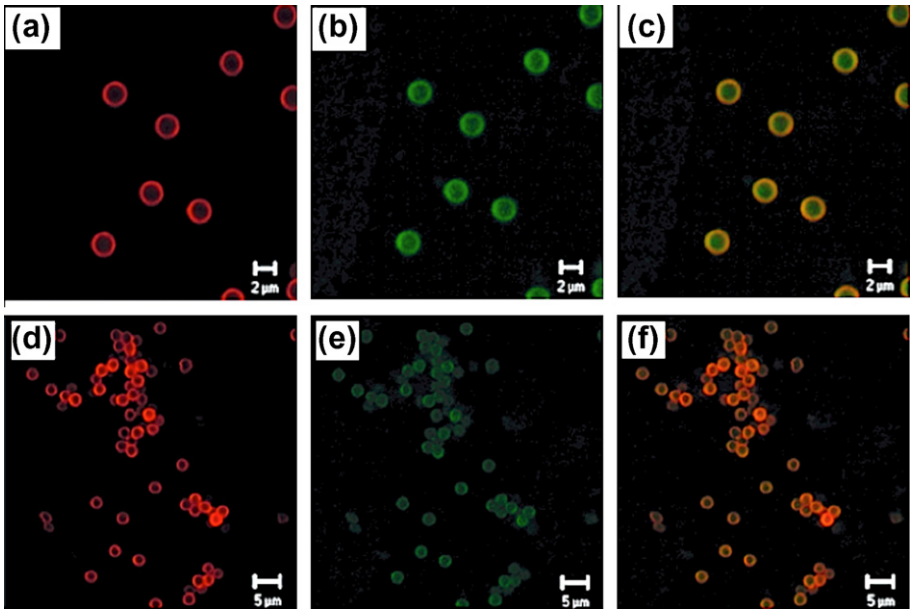

Fig. 5. The CLSM images of hairy/hairy micelle-paired multilayers ((pH 4 $PS_{18.6K}$-*b*-$P4VP_{55.8K}$ with nile red/pH 4 $PS_{4.3K}$-*b*-$PAA_{19.5K}$ with coumarin 30)$_3$) deposited onto PS colloids (a–c) and after the removal of PS colloids ((d–f)). In this case, (a and b) are the fluorescence images of BCM multilayer-coated colloids measured at two different excitation wavelengths of 547 nm (for nile-red) and 400 nm (for coumarin 30), respectively. On the other hand, (d) and (e) are the fluorescence images of BCM hollow capsules measured at two different excitation wavelengths of 547 nm (for nile-red) and 400 nm (for coumarin 30), respectively. In addition, the overlaid images of (a)/(b) and (d)/(e) are shown in (c and f), respectively.

readily dissolved in THF selected to remove the PS colloids, the high degree of intermicellar entanglements between the hairy corona block chains seems to prevent the disruption of PS block cores containing fluorescent dyes during THF treatment for template removal as well as the swelling of PS block cores, thus significantly enhancing the chemical stability of hollow capsules. We also note that the BCM multilayers did not show any fluorescence resonance energy transfer (FRET) despite the partial spectral overlap between the emission spectrum of coumarin 30 (donor) and the absorption spectrum of nile-red (acceptor) (see Supporting information, Fig. S5). This indicates that the FRET is effectively suppressed by the corona entanglement gap between the PS core blocks of $PS_{18.6K}$-*b*-$P4VP_{55.8K}$ and $PS_{4.3K}$-*b*-$PAA_{19.5K}$.

Another intriguing feature to note is that the physical and chemical stability of hollow capsules should also be considered in view of the relative M_W ratio between hydrophobic core and hydrophilic corona blocks. For example, although the degree of electrostatic interaction between $P4VP_{42K}$ and $PAA_{40.2K}$ homopolymer chains in the (PS_{124K}-*b*-$P4VP_{42K}$ (crew-cut)/$PS_{1.4K}$-*b*-$PAA_{40.2K}$ (hairy))$_3$ pair would be much higher in bulk solution than the interaction between $P4VP_{42.4K}$ and $PAA_{19.5K}$ homopolymers in the $PS_{10.6K}$-*b*-$P4VP_{42.4K}$ (hairy)/$PS_{4.3K}$-*b*-$PAA_{19.5K}$ (hairy) micellar pair, the physical and chemical stabilities of hollow (PS_{124K}-*b*-$P4VP_{42K}$/$PS_{1.4K}$-*b*-$PAA_{40.2K}$)$_3$ multilayers were relatively low when compared with those of the hairy/hairy micelle paired multilayers, as shown in the fluorescent images (see Supporting information, Fig. S6). This implies that the degree of intermicellar entanglements to secure the physical stability of hollow micellar capsules is, in fact, the electrostatic interaction between oppositely charged corona block brushes emanating from the PS block cores and it is thus expected that the intermicellar entanglements are also strongly affected by the size of PS block cores, which is, in turn, related to the relative M_W ratio between corona and core block chains of a block copolymer. Also, when the M_W of PS block cores is too small, the aggregation number (i.e., the number of block copolymer chains per micelle) of the micelles is quite low, capturing much less amount of fluorescent dyes within the PS cores and also easily releasing the dyes upon the swelling of PS block cores by THF treatment.

4. Conclusions

The degree of intermicellar entanglements between oppositely charged P4VP and PAA corona block chains, which can be tuned by the deposition pH combination as well as the relative M_W ratio or composition of block copolymer micelles (BCMs), have a significant effect on the physical and chemical stabilities of resulting hollow capsules (based on the hairy/hairy BCM-paired, crew-cut/hairy BCM-paired, and crew-cut/crew-cut BCM-paired multilayers) after removing the PS colloidal templates by THF treatment. In the present study, the hairy/hairy micelle-paired hollow capsules, deposited in the pH 4/4 combination, yielded well-defined BCM multilayer films with small dimple textures on the surface due to the relatively low charge density (i.e., 42% for P4VP and 18% for PAA) as well as the high degree of electrostatic intermicellar entanglements between P4VP and PAA corona block chains. The hairy micelle-paired multilayer hollow capsules show superb physical and chemical stabilities against external stimuli introduced during the removal of PS colloidal substrates by THF treatment. On the other hand, the use of crew-cut micelle pairs with large core size and small corona thickness reduces the electrostatic intermicellar interactions between neighboring micelles, disrupting the BCM multilayers during the removal process of PS colloidal templates. Based on the results obtained in the present study using a number of different combinations of hairy and crew-cut micelles, it is believed that the approach shown here could provide a basis for designing hollow capsules with multiple functions, taking full advantages of hydrophobic BCM nano-scale cores as well as hollowed micron-scale centers.

Acknowledgments

This work was financially supported by the National Research Foundation of Korea Grant funded by the Korean Government (MEST) (The National Creative Research Initiative Program for "Intelligent Hybrids Research Center" (2010-0018290), (NRF-2009-0093282), and the Brain Korea 21 Program, and the WCU (World Class University) Program of Chemical Convergence for Energy and Environment (R31-10013) in SNU Chemical Engineering. Additionally, this work was supported by KOSEF Grant funded by the Korea government (MEST) (2010–0029106, 2009–0085070), and ERC Program of NRF Grant funded by the Korea government (MEST) (R11-2005-048-00000-0). We are also grateful to Mr. Hyomin Lee and Ms. Misook Lee for experimental assistance and Dr. Sewon Oh for helpful discussions.

Appendix A. Supplementary material

Supplementary data associated with this article can be found, in the online version, at doi:10.1016/j.jcis.2011.08.012.

References

[1] E. Donath, G.B. Sukhorukov, F. Caruso, S.A. Davis, H. Mohwald, Angew. Chem. Int. Ed. 37 (1998) 2202.
[2] F. Caruso, Adv. Mater. 13 (2001) 11.
[3] F. Caruso, X.Y. Shi, R.A. Caruso, A. Susha, Adv. Mater. 13 (2001) 740.
[4] F. Caruso, R.A. Caruso, H. Mohwald, Science 282 (1998) 1111.
[5] F. Caruso, W.J. Yang, D. Trau, R. Renneberg, Langmuir 16 (2000) 8932.
[6] X.L. Xu, S.A. Asher, J. Am. Chem. Soc. 126 (2004) 7940.
[7] C.L. Gao, Y.Y. Liang, M. Han, Z. Xu, J.M. Zhu, J. Phys. Chem. C 112 (2008) 9272.
[8] M.M. Titirici, M. Antonietti, A. Thomas, Chem. Mater. 18 (2006) 3808.
[9] J.S. Hu, Y.G. Guo, H.P. Liang, L.J. Wan, C.L. Bai, Y.G. Wang, J. Phys. Chem. B 108 (2004) 9734.
[10] T. Nakashima, N. Kimizuka, J. Am. Chem. Soc. 125 (2003) 6386.
[11] K.P. Johnston, K.L. Harrison, M.J. Clarke, S.M. Howdle, M.P. Heitz, F.V. Bright, C. Carlier, T.W. Randolph, Science 271 (1996) 624.
[12] G. Decher, Science 277 (1997) 1232.
[13] H. Hattori, Adv. Mater. 13 (2001) 51.
[14] J. Hiller, J.D. Mendelsohn, M.F. Rubner, Nat. Mater. 1 (2002) 59.
[15] J. Cho, J.F. Quinn, F. Caruso, J. Am. Chem. Soc. 126 (2004) 2270.
[16] J. Cho, K. Char, J.D. Hong, K.B. Lee, Adv. Mater. 13 (2001) 1076.
[17] F.C. Cebeci, Z.Z. Wu, L. Zhai, R.E. Cohen, M.F. Rubner, Langmuir 22 (2006) 2856.
[18] D. Lee, Z. Gemici, M.F. Rubner, R.E. Cohen, Langmuir 23 (2007) 8833.
[19] S.G. Yang, Y.J. Zhang, G.C. Yuan, X.L. Zhang, J.A. Xu, Macromolecules 37 (2004) 10059.
[20] A.P.R. Johnston, E.S. Read, F. Caruso, Nano Lett. 5 (2005) 953.
[21] J. Seo, J.L. Lutkenhaus, J. Kim, P.T. Hammond, K. Char, Macromolecules 40 (2007) 4028.
[22] B.S. Kim, H. Lee, Y.H. Min, Z. Poon, P.T. Hammond, Chem. Commun. 28 (2009) 4194.
[23] I. Erel-Unal, S.A. Sukhishvili, Macromolecules 41 (2008) 8737.
[24] S. Lee, B. Lee, B.J. Kim, J. Park, M. Yoo, W.K. Bae, K. Char, C.J. Hawker, J. Bang, J. Cho, J. Am. Chem. Soc. 131 (2009) 2579.
[25] Y. Tian, Q. He, C. Tao, J.B. Li, Langmuir 22 (2006) 360.
[26] Y.J. Kang, T.A. Taton, Angew. Chem. Int. Ed. 44 (2005) 409.
[27] Y.J. Kang, K.J. Erickson, T.A. Taton, J. Am. Chem. Soc. 127 (2005) 13800.
[28] B.S. Kim, J.M. Qiu, J.P. Wang, T.A. Taton, Nano Lett. 5 (2005) 1987.
[29] N. Ma, Y.P. Wang, B.Y. Wang, Z.Q. Wang, X. Zhang, G. Wang, Y. Zhao, Langmuir 23 (2007) 2874.
[30] S.I. Yoo, S.J. An, G.H. Choi, K.S. Kim, G.C. Yi, W.C. Zin, J.C. Jung, B.H. Sohn, Adv. Mater. 19 (2007) 1594.
[31] Y. Zhu, W.J. Tong, C.Y. Gao, H. Mohwald, Langmuir 24 (2008) 7810.
[32] J. Cho, J. Hong, K. Char, F. Caruso, J. Am. Chem. Soc. 128 (2006) 9935.
[33] B. Qi, X. Tong, Y. Zhao, Macromolecules 39 (2006) 5714.
[34] J. Hong, W.K. Bae, H. Lee, S. Oh, K. Char, F. Caruso, J. Cho, Adv. Mater. 19 (2007) 4364.
[35] S. Biggs, K. Sakai, T. Addison, A. Schmid, S.P. Armes, M. Vamvakaki, V. Butun, G. Webber, Adv. Mater. 19 (2007) 247.